

Thermal cycling of stress-induced martensite for high-performance shape memory effect

Riccardo Casati,^{a,b,*} Maurizio Vedani^b and Ausonio Tuissi^a

^aCNR-IENI, National Research Council of Italy, Institute for Energetics and Interphases, Corso Promessi Sposi, 29 Lecco, Italy

^bDepartment of Mechanical Engineering, Politecnico di Milano, Via La Masa, 1 Milano, Italy

Received 11 December 2013; revised 3 February 2014; accepted 5 February 2014

Available online 12 February 2014

A novel approach to achieve an extraordinary high stress recovery shape memory effect based on thermal cycling of stress-induced martensite is proposed. An alternative thermodynamic path is considered in order to achieve outstanding functional properties of Ni-rich NiTi alloys, which are commonly used at room or body temperature as superelastic materials. Fatigue tests revealed excellent stability of the material subjected to the novel thermomechanical path, confirming its suitability for employment in high-performance shape memory actuators.

© 2014 Acta Materialia Inc. Published by Elsevier Ltd. All rights reserved.

Keywords: Shape memory alloys; NiTi alloys; Shape memory actuators; High-performance shape memory effect; Stress-induced martensite

Shape memory alloys (SMAs) are smart materials that can recover high deformations by means of a diffusionless solid-phase transformation, known as the martensitic transformation (MT), from a crystallographically higher-symmetry parent phase (austenite) to a lower-symmetry product phase (martensite). The MT is generally characterized by four temperatures, termed martensite finish (M_f), martensite start (M_s), austenite finish (A_f) and austenite start (A_s). The MT can be reversibly induced either by changing the temperature across the transformation temperature range or by applying a stress exceeding a critical value to the austenitic material at constant temperature above A_f . Both martensite and austenite coexist within the temperature range $M_f < T < M_s$ when the material is cooled down from a $T > A_f$, and they also coexist within the range $A_s < T < A_f$ when the material is heated up from a $T < M_f$ [1–3]. A mechanical load applied to a shape memory metal stabilizes the martensitic structure and leads to an increase in the transition temperatures. The Clausius–Clapeyron law describes the behavior accu-

ately. So far, SMAs have been generally categorized into two distinct groups according to their thermodynamically stable phase in the absence of load at environmental temperature [1–5].

The first group includes those alloys exhibiting a martensitic phase at environmental temperature ($T < M_f$), such as the widely employed Ti-rich NiTi intermetallic. These kinds of alloys exploit the so-called shape memory effect (SME). When a stress above a critical value (σ_{DTW}) is applied to these materials, the deformation proceeds via twin boundary movements. The self-accommodated martensite structure, which is characterized by multiple variants, turns into the few most favorable ones. These variants give the largest strain under the given stress condition and grow at the expense of the others. The resulting structure is known as detwinned martensite. Next, upon heating above A_f , the martensite is completely converted to the parent phase and the imposed strain as well as the macroscopic geometrical shape are fully recovered. The SME is schematically depicted in Figure 1 as a solid line. Finally, if the material is cooled below M_f , the resulting structure consists of a self-accommodated martensite. The SME is widely exploited for actuators and microactuators [6–9]. Indeed, if free recovery to the original shape is prevented by a bias load, a recovery stress is produced which can

* Corresponding author at: Department of Mechanical Engineering, Politecnico di Milano, Via La Masa, 1 Milano, Italy. Tel.: +39 0223998638; e-mail: riccardo.casati@polimi.it

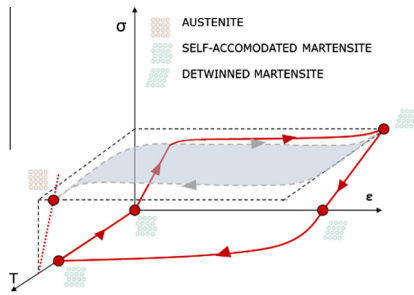


Figure 1. Schematic view of the shape memory effect (SME) (thermo-mechanical loop, solid line) and of the low-force actuator based on the SME (thermal loop under low constant stress, dashed line).

be exploited as actuating force (Fig. 1, dashed line loop) [1–12].

The second group, including the widely employed Ni-rich NiTi compound, consists of pseudoelastic or superelastic materials which show an austenitic phase at environmental temperature ($T > A_f$). This kind of alloy exploits the so-called superelastic effect (SE). If a SMA in the austenitic phase is loaded above a critical stress (σ_{LSE}), then MT is induced. Again, a rough linear relationship, consistent with the Clausius–Clapeyron law, is expected between the critical stress σ_{LSE} and the start temperature (M_s) [4,5]. In this case, the driving force of the transformation is the applied stress. The martensite produced by this kind of crystal transformation is called stress-induced martensite (SIM). Upon unloading, at a critical stress ($\sigma_{USE} < \sigma_{LSE}$), owing to the instability of the martensite at environmental temperature, the reverse phase transformation occurs and a hysteretic mechanical behavior is therefore exhibited (Fig. 2, solid line loop). SE alloys are widely used in the biomedical field, e.g. as vascular stents, and in damping applications [1–4,13–17]. Since the discovery of SMAs, both the SE and SME have been widely studied and considerable research on their fundamentals and engineering aspects have been reported in the open literature [3,10,18–20].

In this work, a novel approach to exploit SMAs is proposed. An alternative thermodynamic path, which allows exceptionally high functional properties to be achieved, is suggested and tested experimentally. It is reported here for the first time that austenitic alloys, which are employed as superelastic materials, can successfully be employed as SMAs for actuators by heating/cooling

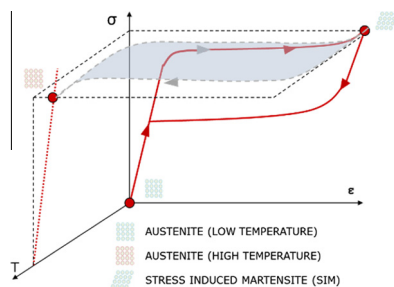


Figure 2. Schematic view of the superelastic effect (SE) (mechanical loop, solid line) and of the high-force actuator based on heating/cooling of stress-induced martensite (HP SME) (thermal loop under high constant stress, dashed line).

cycles starting from SIM. In other words, when loading an austenitic material above a critical stress (σ_{LSE}), SIM is induced and the material deformation proceeds at almost constant stress (superelastic plateau). As the SIM is heated above A_f under constant applied force, it shrinks back due to the stabilization of the austenite. Indeed, since reverse MT takes place, a fully austenitic structure is generated and the macroscopic deformation is therefore recovered. Finally, as the material is cooled down to the environmental temperature, a complete SIM state is reproduced and the deformation is restored (Fig. 2, dashed line loop). To distinguish this newly observed effect based on the thermal cycling of SIM from the conventional SME (i.e. SME based on the heating/cooling of detwinned martensite), we referred to it as the high-performance shape memory effect (HP-SME).

Near-equiatomic NiTi intermetallic compounds are the most widely employed SMA systems for technological application because of their relatively good ductility, low cost and thermomechanical stability.

It is well known that chemical composition is a fundamental parameter to be considered for the design of SMA transformation temperatures. In Ti-rich alloys, characteristic temperatures are almost composition independent. On the other hand, in Ni-rich alloys an increase in Ni content causes a strong drop of MT characteristic temperatures [1–3,21]. Conventional Ti-rich near-equiatomic Ni–Ti wires used for actuators (such as Ni₄₉Ti₅₁) show a fully martensitic structure at room temperature and detwinning tensile stress level of ~100–250 MPa. Conventional SMA actuators usually work in this stress range, as is also suggested by producers of these devices [1–12,22,23].

On the contrary, austenitic Ni-rich NiTi systems show SIM critical stresses up to 1 GPa. Thus, using these materials as actuators according to the proposed scheme, their higher plateau stress level can be exploited in order to produce very high work output.

Ni₄₉Ti₅₁ and Ni_{50.8}Ti_{49.2} (at.%) were melted in a vacuum induction melting furnace (Balzers VSG10) in a controlled argon atmosphere starting from pure elements [24]. The two ingots (70 × 70 × 160 mm³) were hot forged, hot rolled and cold drawn down to the shape of wires 80 μm in diameter. The last thermal treatment (shape setting) of Ni₄₉Ti₅₁ was performed at 400 °C applying an axial stress, while the shape setting of Ni_{50.8}Ti_{49.2} was carried out at 530 °C. After annealing both the wires were water quenched. The transformation temperatures of the two materials were checked by differential scanning calorimetry (Seiko DSC220C) at a scanning rate of 10 °C min^{−1}. A_f temperatures of 65 and 5 °C were detected for martensitic Ni₄₉Ti₅₁ and austenitic Ni_{50.8}Ti_{49.2}, respectively.

The wires were quasi-statically thermomechanically tested using a TA Instrument Q800 dynamical mechanical thermal analyser equipped with tension clamp for uniaxial tests. Martensitic Ni₄₉Ti₅₁ and austenitic Ni_{50.8}Ti_{49.2} specimens 30 mm in length were used to perform the tests. The martensitic wire was loaded up to 250 MPa (above the detwinning critical stress) while austenitic wire was loaded up to 800 MPa (above the superelastic plateau). These wires were then subjected to a thermal cycle holding the maximum applied load

to promote the SME and HP-SME, respectively, at a heating/cooling rate of $2\text{ }^{\circ}\text{C min}^{-1}$.

Fatigue tests were performed to evaluate the thermo-mechanical cycling stability using a specifically developed experimental setup. Martensitic $\text{Ni}_{49}\text{Ti}_{51}$ and austenitic $\text{Ni}_{50.8}\text{Ti}_{49.2}$ wires 100 mm in length were vertically positioned and constrained in the system structure by an upper clamp. They were axially loaded by a weight that was fixed to a lower clamp. The clamps were connected to a power source controlled by a NI Labview program to heat the wire by a step electrical pulse (Joule effect). This program provided a fast control mode of wire deformation: the current was switched off when the sample recovered a strain value of 4% to avoid overheating of the samples. The displacement was measured by a linear voltage differential transducer (Macro Sensors HSTA 750-125). Details of the cycling apparatus are reported elsewhere [25,26]. Thermomechanical cycling up to 6000 cycles under a constant stress of 250 MPa for $\text{Ni}_{49}\text{Ti}_{51}$ wire and of 800 MPa for $\text{Ni}_{50.8}\text{Ti}_{49.2}$, was performed.

The results obtained from quasi-static thermomechanical tests performed on $\text{Ni}_{50.8}\text{Ti}_{49.2}$ thin wires are depicted in the stress–strain–temperature diagram shown in Figure 3a. The curve, which is the result of four thermomechanical steps, clearly shows the functioning of a HP-SME. The austenitic wire was axially loaded at room temperature up to the superelastic plateau (step AB), which was reached at the critical stress of 700 MPa. Then, the SIM was completely induced and the wire was loaded up to the maximum stress of 800 MPa (step BC). Subsequently, the material was heated up to $120\text{ }^{\circ}\text{C}$, under a constant stress of 800 MPa, as depicted in step CD of Figure 3a. In step CD, the austenite phase is restored due to the increase in temperature; the SIM therefore shrunk back and a deformation of 6% was rapidly recovered as temperature reached $95\text{ }^{\circ}\text{C}$. An overheating up to $120\text{ }^{\circ}\text{C}$ was used to ensure full recovery. Finally the material was cooled down to room temperature under a constant stress of 800 MPa (step DC) and the deformation was restored due to the release of SIM as the temperature decreases. Steps CD and DC, which correspond to the heating/cooling cycle under constant load, could be reversibly repeated and a cycling strain recovery of the order of 6% at a stress value of 800 MPa was achieved.

For a direct comparison, the experimental results of the thermomechanical SME test performed on $\text{Ni}_{49}\text{Ti}_{51}$

thin wire are plotted in the graph of Figure 3b using the same axis scale as used in Figure 3a. These experimental curves show the typical functioning of a conventional shape memory actuator based on heating/cooling of the detwinned martensite under a constant bias force. Referring to Figure 3b, during step AB, the martensite wire was axially loaded at room temperature up to 250 MPa. Holding the applied load, a heating/cooling thermal loop (steps BC and CB) was performed between room temperature and $170\text{ }^{\circ}\text{C}$.

The results of Figure 3 demonstrate that within the same temperature range an austenitic $\text{Ni}_{50.8}\text{Ti}_{49.2}$ alloy can be used as an actuator at much higher working stresses (800 MPa) with respect to those used for conventional actuators based on martensitic $\text{Ni}_{49}\text{Ti}_{51}$ alloy (250 MPa). It is worth noting that if an axial stress of 800 MPa is applied to a martensitic Ti-rich NiTi wire, huge plastic deformation would be induced and, often, its ultimate tensile strength would be reached [27]. Moreover, in reference to Figure 3, the two materials show the typical hysteresis loops in the strain–temperature plane. Direct and inverse transformations of Ni-rich austenitic wire occur sharply with $A_s = 88\text{ }^{\circ}\text{C}$, $A_f = 89\text{ }^{\circ}\text{C}$, $M_s = 38\text{ }^{\circ}\text{C}$ and $M_f = 34\text{ }^{\circ}\text{C}$ upon heating and cooling, respectively. Conversely, the characteristic temperatures of the martensitic wire under constant load are much more broadened ($M_s = 90\text{ }^{\circ}\text{C}$, $M_f = 54\text{ }^{\circ}\text{C}$, $A_s = 89\text{ }^{\circ}\text{C}$ and $A_f = 130\text{ }^{\circ}\text{C}$). Again, maximum recovery strain values of 6.2 and 5.8% and thermal hysteresis of 50 and $31\text{ }^{\circ}\text{C}$ were measured for the $\text{Ni}_{50.8}\text{Ti}_{49.2}$ and $\text{Ni}_{49}\text{Ti}_{51}$, respectively.

Thus, novel high-performance shape memory actuators based on the HP-SME can be designed with lower diameters according to their critical stress for inducing SIM. This implies further technological advantages such as shorter actuation time, shorter restoring time, lower amperage, lower energy consumption and overall smaller dimensions. All the aforementioned properties are of major importance in actuator design, in particular for SMA actuators applications in consumer electronics. However, it is also necessary to consider that wires with smaller diameter are more difficult to crimp and fasten to the structure.

Thermomechanical fatigue tests of wire specimens were performed through heating with current pulses a vertically positioned wire subjected to a constant load, using an apparatus reported elsewhere [25,26]. As shown in Figure 4, for both austenitic and martensitic wires,

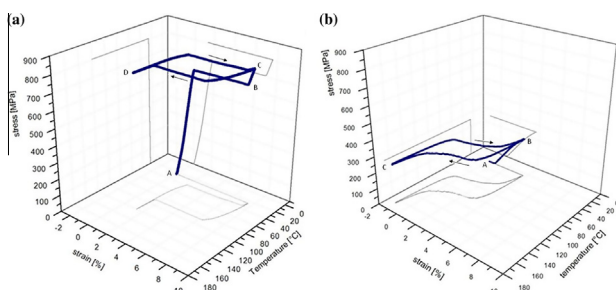


Figure 3. Thermomechanical tests performed on: (a) austenitic $\text{Ni}_{50.8}\text{Ti}_{49.2}$ (HP-SME) and (b) martensitic $\text{Ni}_{49}\text{Ti}_{51}$ (SME).

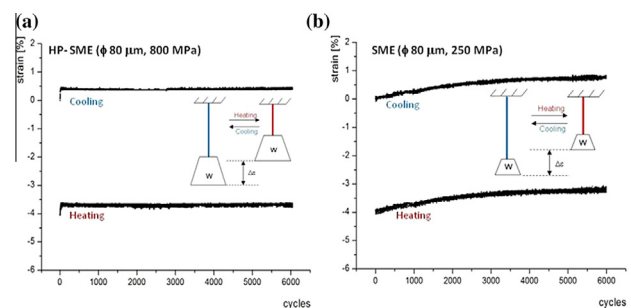


Figure 4. Fatigue test performed on: (a) austenitic $\text{Ni}_{50.8}\text{Ti}_{49.2}$ (HP-SME); (b) martensitic $\text{Ni}_{49}\text{Ti}_{51}$ (SME).

the minimum and maximum wire deformation values were measured and plotted as a function of the number of cycles (Fig. 4a,b, respectively).

Martensitic wire (Fig. 4b) accumulates irreversible plastic deformation during all 6000 cycles ($\sim 0.8\%$) at 250 MPa. The fatigue behavior of austenitic wire under 800 MPa is completely different (Fig. 4a). The high stress level leads to the accumulation of plastic deformation in the first few thermomechanical cycles ($\sim 0.4\%$), then the material exhibits an excellent cyclic stability since no further considerable irreversible deformation is induced. The high stress likely leads to an earlier steady-state hysteresis loop (ϵ - T): fewer thermomechanical cycles are then needed to stabilize the functional properties. Therefore, a preliminary thermomechanical cycling may avoid the accumulation of plastic deformation during the working life of a device, and therefore the training procedure for stabilizing the functional properties of materials used for prolonged applications might be simplified.

To conclude, although austenitic SMAs have been well known for a few decades, they have so far been commonly used at environmental temperature as super-elastic materials. Nevertheless, they have never been employed by exploiting their SME. In this work, an unconventional thermodynamic path, which occurs between low-temperature SIM and high-temperature austenite, has been suggested, and has been proven to be suitable in exploiting SE austenitic alloy to produce an exceptionally high mechanical work. The experimental results show that, by exploiting this novel path, strains of the order of 6% can be reversibly recovered while a very high bias stress is applied (800 MPa). Preliminary fatigue tests revealed an excellent stability up to 6000 cycles of the material subjected to the cooling/heating of SIM, confirming that this thermomechanical path is suitable for the design of high-performance shape memory actuators based on the HP-SME.

The authors would like to thanks Enrico Bassani, Marco Pini and Giordano Carcano of CNR IENI Lecco Unit for their technical assistance in NiTi processing.

- [1] K. Otsuka, X. Ren, *Prog. Mater. Sci.* 50 (2005) 511–678.
- [2] K. Otsuka, C.M. Wayman, *Shape Memory Materials*, Cambridge University Press, Cambridge, 1998.

- [3] T. Owen, *Robotica* 6 (1988), 259–259.
- [4] P. Wollants, M. Bonte, J.R. Roos, *Z. Metalk.* 70 (1979) 113.
- [5] J. Olbricht, A. Yawny, J.L. Pelegrina, A. Dlouhy, G. Eggeler, *Metall. Mater. Trans.* 42A (2011) 2556–2574.
- [6] M. Kohl, K.D. Skrobaneck, *Sens. Actuators, A* 70 (1998) 104–111.
- [7] M. Kohl, K.D. Skrobaneck, E. Quandt, P. Schlobmacher, A. Schiialer, D.M. Allen, *J. Phys. IV C8* (1995) 1187–1192.
- [8] M. Kohl, *Shape Memory Actuators*, Springer Verlag, Berlin, 2004.
- [9] C. Grossmann, J. Frenzel, V. Sampath, T. Depka, G. Eggeler, *Metall. Mater. Trans.* 40A (2009) 2530–2544.
- [10] J. Van Humbeeck, *Mater. Sci. Eng., A* 273 (275) (1999) 134–148.
- [11] R. Casati, A. Tuissi, S. Belochapkin, C. Dickinson, S. Tofail, *Funct. Mater. Lett.* 5 (2012) 1250009.
- [12] D. Reynaerts, H. Van Brussel, *Mechatronics* 8 (1998) 635–656.
- [13] A. Tuissi, P. Bassani, R. Casati, M. Bocciolone, M. Carnevale, A. Collina, A. Lo Conte, B. Previtali, *JMEP* 18 (2009) 612–619.
- [14] J. San Juan, M.L. No, C.A. Schuh, *Nat. Nanotechnol.* 4 (2009) 415–419.
- [15] X. Wang, C. Li, B. Verlinden, J. Van Humbeeck, *Scripta Mater.* 69 (2013) 545–548.
- [16] C. Maletta, E. Sgambitterra, F. Furguele, R. Casati, A. Tuissi, *Smart Mater. Struct.* 21 (2012) 112001.
- [17] T. Duerig, A. Pelton, D. Stockel, *Mater. Sci. Eng., A* 273 (275) (1999) 149–160.
- [18] S. Miyazaki, Y. Igom, K. Otsuka, *Acta Metall.* 34 (10) (1986) 2045–2051.
- [19] S. Miyazaki, K. Otsuka, Y. Suzuki, *Scripta Metall.* 15 (1981) 287–292.
- [20] J.A. Shaw, S. Kiriakides, *J. Mech. Phys. Solids* 43 (8) (1995) 1243–1281.
- [21] J. Frenzel, E.P. George, A. Dlouhy, Ch. Somsen, M.F.-X. Wagner, G. Eggeler, *Acta Mater.* 58 (2010) 3444–3458.
- [22] <http://www.nitinol.com/wp-content/uploads/2012/01/Material-Data-Sheet-Shape-Memory.pdf>.
- [23] [http://www.saesgetters.com/sites/default/files/SmartFlex Wire & Spring datasheets_1.pdf](http://www.saesgetters.com/sites/default/files/SmartFlexWire%20Spring%20datasheets_1.pdf).
- [24] S. Besseghini, A. Tuissi, E. Olzi, F. Cito, G. Carcano, *Vuoto Sci. Technol.* 26 (1997) 5–9.
- [25] R. Casati, F. Passaretti, A. Tuissi, *Proc. Eng.* 10 (2011) 3423–3428.
- [26] R. Casati, A. Tuissi, *JMEP* 21 (2012) 2633–2637.
- [27] K.N. Melton, O. Mercier, *Acta Metall.* 29 (2) (1981) 393–398.